IOPscience iopscience.iop.org

Home Search Collections Journals About Contact us My IOPscience

Piezoelectric transducer design for a miniaturized injectable acoustic transmitter

This content has been downloaded from IOPscience. Please scroll down to see the full text.

2015 Smart Mater. Struct. 24 115010

(http://iopscience.iop.org/0964-1726/24/11/115010)

View the table of contents for this issue, or go to the journal homepage for more

Download details:

IP Address: 130.20.72.148
This content was downloaded on 18/02/2016 at 22:56

Please note that terms and conditions apply.

OPEN ACCESS
IOP Publishing
Smart Materials and Structures
Smart Mater. Struct. **24** (2015) 115010 (9pp)
doi:10.1088/0964-1726/24/11/115010

Piezoelectric transducer design for a miniaturized injectable acoustic transmitter

H Li, K W Jung and Z D Deng

Pacific Northwest National Laboratory, PO Box 999, Richland, WA 99352, USA

E-mail: zhiqun.deng@pnnl.gov

Received 20 February 2015, revised 30 June 2015
Accepted for publication 25 August 2015
Published 7 October 2015

Abstract

Implantable acoustic transmitters have been used in the last 20 years to track fish movement for fish survival and migration behavior studies. However, the relatively large weights and sizes of commercial transmitters limit the populations of studied fish. The surgical implantation procedures may also affect fish adversely and incur a significant amount of labor. Therefore, a smaller, lighter, and injectable transmitter was needed, and similar or better acoustic performance and service life over those provided by existing commercial transmitters was desired. To develop such a small transmitter, a number of technical challenges, including design optimization of the piezoelectric transducer, needed to be overcome. Our efforts to optimize the transducer focused on improving the average source level in the 180° range in which the signal was not blocked by the transmitter body. We found that a novel off-center tube transducer improved the average source level by 1.5 dB. An acoustic reflector attached to the back of the transducer also improved the source level by 1.3 dB. We found that too small a gap between the transducer and the component placed behind it resulted in distortion of the beam pattern. Lastly, a tuning inductor in series with the transducer was used to help optimize the source level. The findings and techniques developed in this work contributed to the successful development and implementation of a new injectable transmitter.

Keywords: acoustic transducer, piezoelectric, PZT, underwater acoustic transmitter, fish tag, source level, beam pattern

(Some figures may appear in colour only in the online journal)

1. Introduction

In the past 20 years, salmon recovery and potential detrimental impact of hydroelectric dams on fish survival have been receiving great national attention because of their environmental and economic importance [1–3]. Therefore, it is of great interest to study and understand the behavior of migrating salmonids through river systems and dams so measures to improve the survival rates of these species can be optimized or implemented. Acoustic telemetry has been employed to investigate the movement and migration of juvenile salmon during the last decade [4–6]. Underwater acoustic transmitters have detection ranges of tens to hundreds of meters and do not rely on an antenna for signal transmission, making them ideal for three-dimensional tracking. However, the relatively large sizes of acoustic transmitters limit the populations of fish that can be tagged and studied because of the tag burden imposed on the fish. Therefore, over the last 10 to 20 years, the sizes of acoustic transmitters have been gradually reduced through the development efforts of researchers and commercial fish tag vendors. Through the reductions in transmitter size, tagging of fish as small as juvenile salmon has become a reality. An example is the small transmitter developed for the Juvenile Salmon Acoustic Telemetry System (JSATS), which is a fish monitoring system developed by the US Army Corps of Engineers (USACE), Portland District; Pacific Northwest National Laboratory (PNNL); and National Oceanic and Atmospheric Administration, Fisheries. However, the

Content from this work may be used under the terms of the Creative Commons Attribution 3.0 licence. Any further distribution of this work must maintain attribution to the author(s) and the title of the work, journal citation and DOI.

 © 2015 IOP Publishing Ltd Printed in the UK

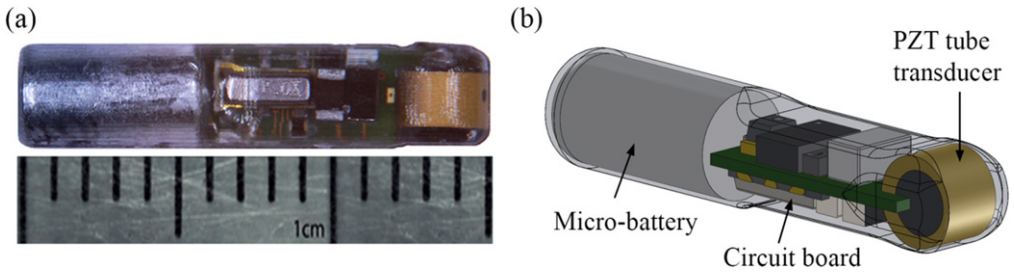

Figure 1. Photograph of the injectable JSATS transmitter (a) and its CAD representation (b).

smallest current JSATS transmitter was 10.7 mm long, 5.0 mm wide, and weighed 300 mg so the newer transmitters were still too big to be implanted in juvenile salmon smaller than 95 mm in length. In addition, extensive handling of the fish was still required, which may negatively bias fish survival measurements and other migratory behavior metrics. Therefore, there has been a need to develop a miniaturized acoustic transmitter that is small enough to be injected with an 8-gauge needle, thus removing the need for surgical implantation and suturing. More importantly, an injectable transmitter would also allow tagging of smaller fish that could not be tagged previously, thereby reducing bias in the experimental results due to the limited size range of fish used in a study.

A typical acoustic fish tag consists of three primary components: (1) a piezoelectric transducer for emitting the acoustic signal that identifies the tagged fish, (2) circuitry that controls the ping rate and frequency of the acoustic signal, and (3) a battery that powers the entire transmitter. The main challenge of developing such an injectable transmitter was how to achieve the same or better acoustic performance and the service life provided by existing transmitters in a much smaller and lighter package, as the reduction in the package size requires a more compact device, a smaller battery, and smaller electrical components that are often less efficient than their larger counterparts.

By improving the designs of all the three primary components of the transmitter, an injectable transmitter (shown in figure 1) was successfully developed by PNNL for JSATS in 2013 [7]. This new transmitter is able to produce an average source level of 155 dB (reference: 1 μPa at 1 m) and has a service life of 130 days at a 3 s ping rate. Its form is mostly cylindrical except for the front half, which is slimmed down slightly to reduce the weight. It is 15.0 mm long, 3.38 mm in diameter (at the backend where the micro-battery is located), and weighs 217 mg. In a field test undertaken immediately after development, the new transmitter demonstrated similar performance and tag life to existing transmitters, and the single-reach survival rates of the tagged fish were significantly better than that of fish tagged with the existing, larger transmitters. Our work on developing the micro-battery specifically for the injectable transmitter has been reported previously [8].

This paper reports the core research conducted to improve and optimize the design of the piezoelectric transducer as a part of the collective development effort for this new transmitter. The optimization techniques of the transducer discussed herein are focused primarily on methods for redirecting the input electrical energy to the transducer toward the directions in which tagged fish are more likely to be detected by the receiving hydrophones.

2. Experimental

2.1. Sample preparations

The piezoelectric tube transducer samples used in the development of the JSATS injectable transmitter were lead zirconate titanate (PZT) ceramic transducers purchased from Morgan Electro Ceramics (Bedford, OH, USA), and TRS Technologies (State College, PA, USA). The bases for the dimensions of the PZT tube transducer used in this study were the application frequency of JSATS (416.7 kHz) and the frequency constant of the PZT. For the electrical and performance characterizations, two thin wires were attached to the inner and outer walls of the transducer using a silver epoxy and then soldered to a coaxial cable that was wrapped in silver-plated copper braiding to shield the RF emission from the cable when the transducer was excited with an alternating current voltage. To waterproof the transducer, the PZT transducer was coated with an approximately 0.1 mm thick layer of hot melt glue.

2.2. Electrical and frequency measurements

The impedance, resonance, and anti-resonance of the PZT transducers were measured using an Aglient 4294A Precision Impedance analyzer (Agilent Technologies, Santa Clara, CA, USA). The resonance and anti-resonance frequencies were identified using the local minimums and maximums in the impedance spectrum. The capacitances of the transducers were measured using an inductance/capacitance/resistance meter (Model 879 B, BK Precision, Yorba Linda, CA, USA).

2.3. Source-level measurements

The source-level measurements were conducted in an acoustic tank at PNNL's Bioacoustics and Flow Laboratory [9], which is accredited by the American Association for Laboratory Accreditation to the ISO/IEC 17025:2005 standard for calibration and testing laboratories. The interior walls, the bottom of the tank, and the bottom of the lid were lined with a 26 mm thick layer of an anechoic material

(Aptflex F48, Precision Acoustics Ltd, Dorchester, Dorset, UK), which minimized the impact of echoes and noises within the tank. The tank was filled with fresh water. The PZT tube transducer samples fabricated using the method described above and a receiving hydrophone (Model SC001-2008-0004, Sonic Concepts, Bothell, WA) with a 10.6 dB gain were submerged into the tank at a depth of 17 in. with a 1 m separation between the PZT and the hydrophone. The tube axis of the PZT was perpendicular to the surface of water. The PZT samples were mounted on a motion control unit so their movement could be controlled three-dimensionally using testing software written in MATLAB (MathWorks, Inc., Natick, MA, USA) installed on a Dell Precision T7500 computer workstation (Dell, Round Rock, TX, USA).

Prior to the measurements being taken, an omnidirectional broadband projector hydrophone (Model TC-4034, Reson A/S, Slangerup, Denmark) was used to calibrate the sensitivity of the receiving hydrophone. An actual JSATS transmitter identification code was used as the input signal for the source-level measurement. The identification code used binary phase shift keying at a frequency of 416.7 kHz and was 31 bits in length, including a 7-bit Barker code, 16 data bits, and 8 cyclic redundancy check bits. The 31-bit code was sent in a square wave at a pulse rate interval from a MATLAB interface through a data acquisition card (Model PCI-6111, National Instruments Corporation, Austin, TX). The source level was calculated using equation (1):

$$SL = 20\log_{10}V_{\mathrm{R}} + TL - S_{\mathrm{R}} - G_{\mathrm{R}}. \quad (1)$$

Here, SL is the source level, V_{R} is the root mean square output voltage of the receiving hydrophone, TL is the transmission loss, S_{R} is the sensitivity of the receiving hydrophone, and G_{R} the gain of the data acquisition system. All the terms in this equation are expressed in decibels.

During source-level and beam-pattern measurements, PZT transducer was initially positioned with the PZT transducer directly facing the receiving hydrophone and the coaxial cable was positioned behind the PZT. During the test, the PZT transducer was rotated in the horizontal plane at 10° intervals through a full 360° circle, with source-level readings taken at every angle, while keeping the receiving hydrophone stationary. The source-level reading was collected three to five times at each angle, and the average of the readings for each angle was used as the final value for each individual angle. The average of all source-level readings of the 180° range in which the PZT directly faced the hydrophone without being blocked by the coaxial cable was used as the representative source-level value (SL_{avg}) for the PZT transducer. This approach was adopted to be consistent with the testing protocol of existing JSATS transmitters in which the acoustic signal is always partially blocked by the circuitry and the battery.

2.4. Finite element analyses (FEA)

The FEA were conducted using COMSOL Multiphysics (version 4.3a) software with the Acoustic Module (COMSOL Inc., Palo Alto, CA, USA). A three-dimensional model of a PZT-5H tube transducer with an outer diameter of 2.54 mm, an inner diameter of 1.75 mm, and a height of 1.75 mm was used. It was assumed that the inside of the PZT tube was filled with air. The PZT tube was excited with a voltage of 8.5 V at 416.7 kHz. The mesh sizes were no greater than 1/6 of the wavelength of the sound wave in the respective medium [10]. The outermost acoustic medium was water, and for simplicity it was modeled as a sphere in the spherical coordinate system. However, due to the high computational cost of modeling the entire far-field interested (i.e., 1 m from the PZT) based on a regular finite element approach, a perfectly matched layer (PML) was introduced to terminate the outermost acoustic medium without introducing any reflection from the PML boundary. The concept of the PML was introduced by Berenger in electromagnetics [11], and it has been widely used in the problem of free-space simulation such as radiation and scattering in acoustics [12–14]. With the implementation of a PML, the sound pressure level at a distance located in the far-field can be calculated by the Helmholtz–Kirchhoff integral theorem [15, 16]. In this study, the water sphere (i.e., the outermost acoustic medium) had a radius of 19.2 mm surrounding the PZT transducer in its center, and this sphere was terminated by the PML that was one wavelength thick in water (i.e. 3.6 mm). Additionally, a boundary layer with the thickness of 0.06 mm was placed between the water sphere and the PML to set the boundary for computing the Helmholtz–Kirchhoff integral equation [12, 13, 15, 16].

2.4.1. FEA for the PZT transducer with an acoustic reflector.

To simulate the beam pattern of the PZT transducer with the reflector, a simplified model consisting of the PZT tube, the reflector and a layer of glue between them were used. As in the case of the actual samples, the reflector was 0.3 mm thick, 2.0 mm wide and 1.75 mm tall. The reflector material used in the model is the built-in closed-cell foam material 'closed-cell foam (solid, 101 kPa)' in COMSOL, as the actual reflector material (EPDM closed-cell foam) was not listed in COMSOL's Material Library. As the acoustic properties of the EPDM closed-cell foam were not available from the vendor, the speed of sound in the form was assumed to be 1200 m s^{-1}. In addition, in the actual experiments the 0.3 mm thick reflector foam was cut from a much larger sheet, some closed cells in the reflector became exposed, which would increase the apparent density of the reflector. Therefore, the density of the reflector in the model was assumed to be 200 kg cm^{-3}, slightly higher than the measured density of the closed-cell foam (130 kg cm^{-3}). No material damping was used in the model. The acoustic-structure boundaries of the model were all the surfaces of the PZT transducer.

2.4.2. FEA for the PZT transducer backed by an inductor with spacing.

The beam patterns of the PZT transducer with and without an inductor placed behind it were simulated. The PZT had air inside, similar to the simulations for the PZT transducer with an acoustic reflector. The inductor was modeled as a rectangular block with the dimension of 2.00 mm × 1.00 mm × 1.25 mm ($w \times h \times d$ with the wh

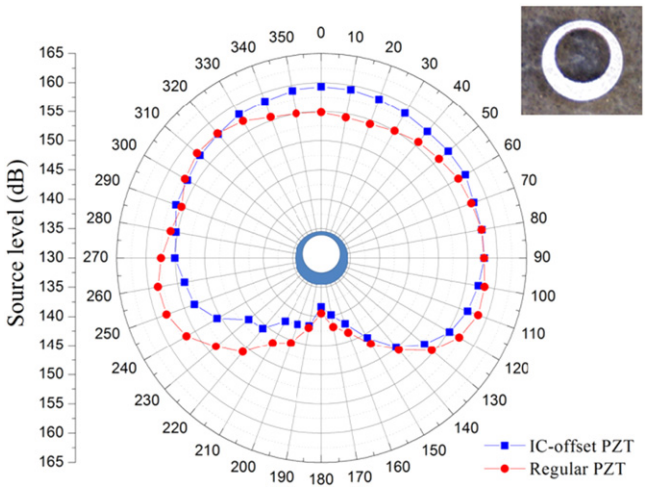

Figure 2. Comparison of the beam patterns of the IC-offset PZT tube and a regular PZT tube of the same dimensions. The off-center tube at the center of the beam pattern indicates the orientation of the IC-offset PZT. The inset shows a photo of an actual IC-offset PZT tube.

face facing the PZT) and was positioned directly behind the PZT transducer with spacing. The selected spacing values between the PZT transducer and the inductor were 0.50, 0.75, and 1.00 mm. For simplicity, the epoxy layer between the PZT and the inductor was neglected in the model based on the fact that the characteristic impedance of the epoxy ($2 \sim 3$ MRayl) is fairly close to that of water (1.5 MRayl). No material damping was used in the model and the acoustic-structure boundaries of the model were all the surfaces of the PZT transducer. Because of the fact that no information on the acoustic properties (i.e., density and speed of sound) of the inductor material was available, the material for the inductor was assumed to be a ceramic. Additionally, because the acoustic impedance of water and ceramics are different by an order of magnitude in general, the surface of the inductor was assumed to be a sound hard boundary.

3. Results and discussion

To maximize the detectability of the tagged fish, an omnidirectional piezoelectric transducer that can emit acoustic signal uniformly in all directions is preferred. The existing acoustic transmitters use a PZT tube transducer instead of a spherical transducer mainly because of the difficulty of manufacturing spherical ceramic transducers at such a small size and the relatively larger weight of the spherical transducer to achieve the same resonance frequency.

The PZT tube transducer operates in the so-called 'hoop' mode, in which the tube vibrates along the radial direction (i.e. the tube circumference vibrates in an expanding–contracting motion) to generate an omnidirectional beam pattern in the planar direction normal to the tube axis of the transducer. PZT ceramics are better suited for this design because of their polycrystalline nature, which enables them to align their dipoles in the radial direction of the tube (i.e., along the wall thickness direction). Although they have superior piezoelectric properties, ferroelectric single crystals such as lead magnesium niobate-lead titanate are not used because of their high cost and, more importantly, the heavy dependence of their piezoelectric properties on the crystal orientation, which would result in significant variation of the acoustic signal strength along the circumference of the tube transducer.

In state-of-the-art acoustic transmitters, the acoustic signal emitted from the PZT transducer is inevitably partially blocked by the circuit board and the battery positioned behind the transducer (figure 1). As a result, the overall beam pattern is actually quasi-omnidirectional. The signal blocking by these components typically results in a 14–18 dB drop in source level, which significantly reduces the detection probability and range of the transmitter. The acoustic signal emitted toward the back of the transmitter is thus considered to be wasted. Therefore, if the acoustic energy could be directed more to the front of the transmitter instead of being emitted uniformly in all directions normal to the wall of the PZT transducer, the efficiency of the transducer would be improved.

3.1. Off-center PZT

When subjected to an applied voltage, the deformation of a piezoelectric material is directly proportional to the amplitude of the electric field, which is voltage per unit length along the direction in which the electric field is applied. Therefore, for a piezoelectric tube transducer that is polarized through the wall thickness direction, if given the same voltage, a tube with a smaller wall thickness is driven harder than one with a thicker wall, and a stronger acoustic signal will result. In existing JSATS transmitters, the tube transducer has a regular tube geometry (i.e., a uniform wall thickness throughout its entire circumference); therefore, it will emit acoustic signals of the same amplitude around the entire wall surface. If a tube transducer with a varying wall thickness along the circumference is used, when the same driving voltage is applied, the portion of the tube with a smaller wall thickness would be driven harder than the portion with a larger wall thickness. As a result, a larger portion of the input electric energy into the transducer would be directed to the thinner portion. If such a tube transducer is used in the transmitter with its thicker portion positioned facing the circuit board, more acoustic energy would be directed away from this direction and the amount of the energy emitted towards the front of the transmitter would be increased compared to a regular tube transducer, leading to a more efficient use of the input electric energy.

A typical way to fabricate piezoelectric ceramic tube transducers is to drill into a solid block of the ceramic. Therefore, by purposely drilling out the inner circumference (IC) of the tube off the center of the outer circumference, a tube transducer with varying wall thickness can be created. PZT tubes using this custom design were ordered and tested against regular PZT tubes that were made from the same material and had the same dimensions (inner diameter [ID] = 1.80 mm, outer diameter [OD] = 2.54 mm and

length = 1.75 mm). The offset of the custom tube was 0.15 mm.

The beam patterns of the IC-offset and regular tube transducers are compared in figure 2. The thinnest portion of the IC-offset tube showed the highest source level as expected, and the front half of the IC-offset tube (the top half of the tube in the figure) showed an average source level 1.5 dB higher than that of the regular tube. This indicates that the energy input into the front half of the transducer was enhanced by approximately 40%.

It is worth noting that the IC-offset geometry does not change the hoop-mode resonance frequency of the PZT tube transducer, as the hoop-mode resonance frequency is only related to the average diameter of the tube, namely (OD + ID)/2, by the frequency constant:

$$f_r = \frac{2N_c}{(\mathrm{OD} + \mathrm{ID})} \tag{2}$$

where N_c is the hoop-mode frequency constant of the PZT material. Shifting the center of the IC does not change either the ID or OD of the tube; therefore, it should not result in a change in f_r. This was confirmed by the impedance spectrum comparison between the IC-offset tube and the regular tube (figure 3). Both transducer samples were made from the same PZT material and had the same OD and ID.

3.2. Effect of an acoustic reflector

Acoustic energy emitted from the rear of the PZT transducer can also be redirected by creating an acoustic impedance mismatch on the surface of the transducer. When an acoustic wave travels through a boundary between two different mediums, reflection and transmission occur at this boundary. The power transmission coefficient T_p, which is defined as the power ratio of the incident wave to the transmitted wave, is related to the acoustic impedances of the two media [17]:

$$T_p = \frac{A_t}{A_i} \frac{4r_2/r_1}{\left(r_2/r_1 + 1\right)^2}, \tag{3}$$

where A_t and A_i are the cross-section areas of the incident and transmitted waves, respectively. The terms r_1 and r_2 are the characteristic impedances of the PZT material and the material directly in contact with the PZT surface, respectively. In our case, A_t and A_i are equal. Thus, one can see that when the two characteristic impedances have similar values, T_p is close to 1. Most of the acoustic energy transmits through the boundary. When r_1 is either far greater or far smaller than r_2, T_p is close to zero, and most of the acoustic energy is reflected at the boundary. Therefore, a material with very low characteristic impedance can be used as a 'reflector' on the surface of the PZT to change the directions in which the acoustic waves travel inside the PZT material.

In the case of the injectable transmitter, because the PZT transducer is a tube operating in the hoop mode, the transducer emits acoustic waves on both the outer and inner wall surfaces. If the inside of the PZT tube is filled with a solid material such as an epoxy, the acoustic waves propagating toward the inside of the tube will be dissipated as heat or will result in destructive interference situations because of the ID of the transducer (1.7 to 1.8 mm) and wavelength of the 416.7 kHz signal, both of which lead to wasted input energy. Thus, it is necessary to place a reflector material inside the PZT to reduce the amount of the inward transmitting acoustic energy.

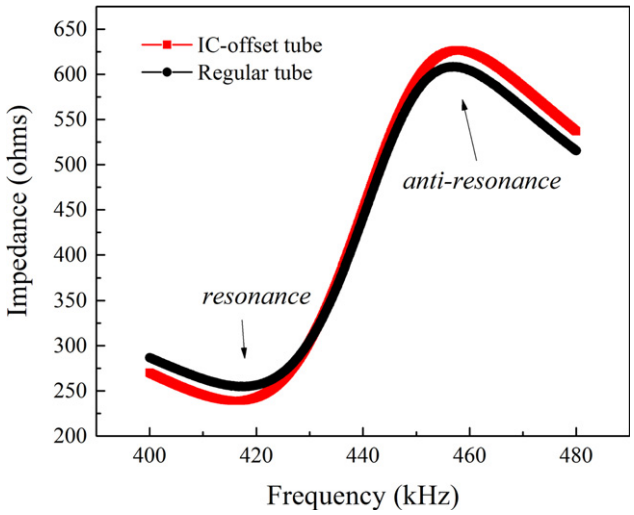

Figure 3. Comparison of the resonance frequencies of the IC-offset PZT tube and a regular PZT tube of the same dimensions.

In a previous study [18], we investigated the source levels of the PZT tube transducers that used four different types of filler materials inside the PZT: (1) CircuitWorks CW2400 silver epoxy, (2) EPO-TEK 301 nonconductive epoxy, (3) hot melt glue, and (4) EPDM (ethylene propylene diene monomer) close-cell foam (EPDM-CCF hereinafter, McMaster-Carr, Aurora, OH, USA). We found that the source level of the tube transducer increased as the density and acoustic impedance decreased, and the difference in the source level could be as large as 7 dB. The EPDM-CCF filler gave the highest source level at 158.5 dB, which satisfied the source-level requirement of the JSATS transmitter. Therefore, EPDM-CCF was chosen as the PZT filler material for the injectable transmitter.

As mentioned in section 3.1, acoustic waves emitted from the rear of the tube transducer are also considered to be wasted from the transmitter's detectability point of view; therefore, it is beneficial to redirect those waves toward the front portion of the tube. In addition to using the IC-offset tube geometry, wave redirection also can be realized by placing a reflector directly behind the PZT.

In this study, a piece of EPDM-CCF approximately 0.3 mm thick was used as the reflector material. Finite element analysis (figure 4) was conducted in the frequency domain using COMSOL Multiphysics to verify the redirection of the acoustic waves due to the presence of the reflector in terms of the source level estimated at 1 m distance from the center of the PZT tube. The simulated beam pattern in figure 4 was obtained from a reflector that had an angular coverage of 90° (i.e. a quarter of the PZT outer wall was covered by the reflector). Compared to the simulation result of the case

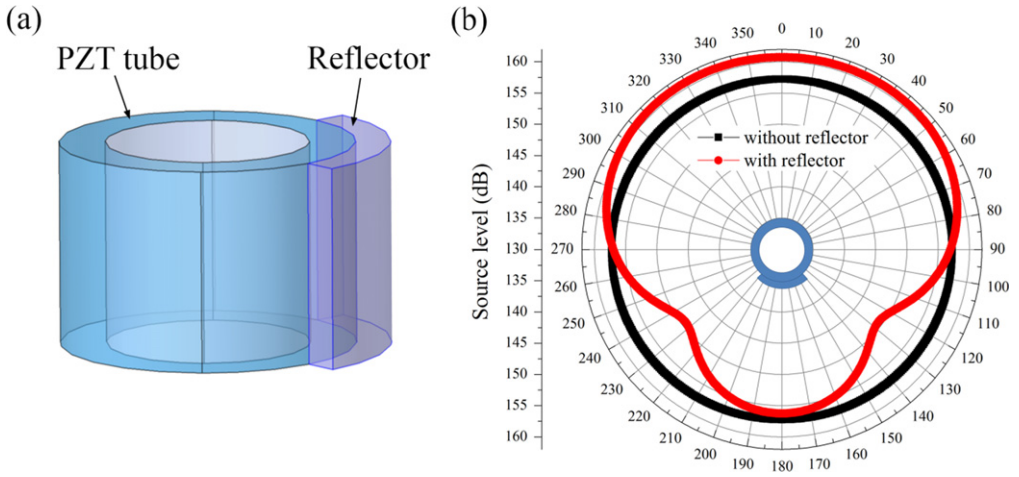

Figure 4. The PZT-reflector model used in the FE analysis (a) and the simulated beam patterns using the models with and without the reflector (b). The tube at the center of the beam pattern indicates the location of the reflector on the PZT.

without the reflector, the reflector redirected the acoustic intensity, which is defined as the power per unit area, toward the frontal angles of 180° (i.e. between 270° and 90°) and helped to enhance the source level by 4.2 dB at 0° (i.e. when the length axis of the transmitter is aligned with the receiving hydrophone). The simulation results show that the reflector enhanced SL_{avg} by as much as 2.9 dB. The source level of the transducer with the reflector started to decrease at 50° (or 310°). The source levels on the sides of the transducer (at 90° and 270°) were 3.8 dB lower than the 0° value.

Actual transducer samples with the reflector were also fabricated and tested for source level (figure 5). The results showed that the presence of a reflector behind the PZT did improve the overall source level in the front half of the beam pattern. In agreement with the simulation results, the sample with the reflector also exhibited a 3 dB source level difference between the 0° value and the 90° (or 270°) value. Compared to the transducer without the reflector, the source level of the transducer with the reflector showed a 3 dB enhancement in source level at 0° instead of the 4.2 dB indicated by the simulation. Additionally, SL_{avg} was only enhanced by 1.3 dB instead of the 2.9 dB given by the simulated results. These discrepancies were probably caused by the facts that: (1) in reality, there is always damping loss within the materials, which was not accounted for in the simulations as no damping data of these materials were available; and (2) the material properties used in the simulation were only estimates because the full sets of material properties required for the simulation were not available. It should be noted that the beam-pattern discrepancy between the simulation and the experimental results in the back side of the PZT was due to the fact that the coaxial cable connected to the PZT in the actual samples was not modeled in the simulation.

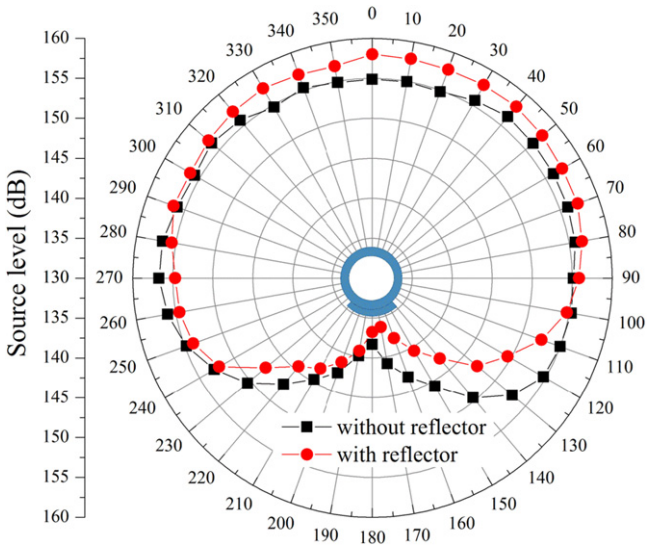

Figure 5. Comparison of the beam patterns of the PZT tube transducer with and without the acoustic reflector. The tube at the center of the beam pattern indicates the location of the reflector on the PZT.

3.3. PZT-component spacing

A typical underwater acoustic transmitter is usually encapsulated in epoxy resin. The speed of sound in an epoxy resin is ~2000 m s^{-1} [19]. Thus, in the case of JSATS, the 416.7 kHz application frequency translates into a wavelength of ~5 mm in an epoxy resin, which is in the same order of magnitude of the 3.4 mm diameter of the transmitter. Moreover, because of the extremely compact placement of the components inside the transmitter body, the spacing between the PZT transducer and the inductor directly behind it is <1 mm. This extremely small spacing may create a complex scattered sound field between the inductor and the transducer. For example, the radiated sound from the PZT is reflected by the inductor and this reflected sound can be then scattered by the PZT. In this event, due to the high frequency the reflected sound toward the PZT will be scattered by the PZT with a significant amount of forward scattering (i.e., toward the forward 180° from the standpoint of the PZT transducer) that may cause constructive or destructive interference with the sound field directly radiating from the PZT. This interference results in fluctuation in the far-field sound pressure and, consequently, a distorted

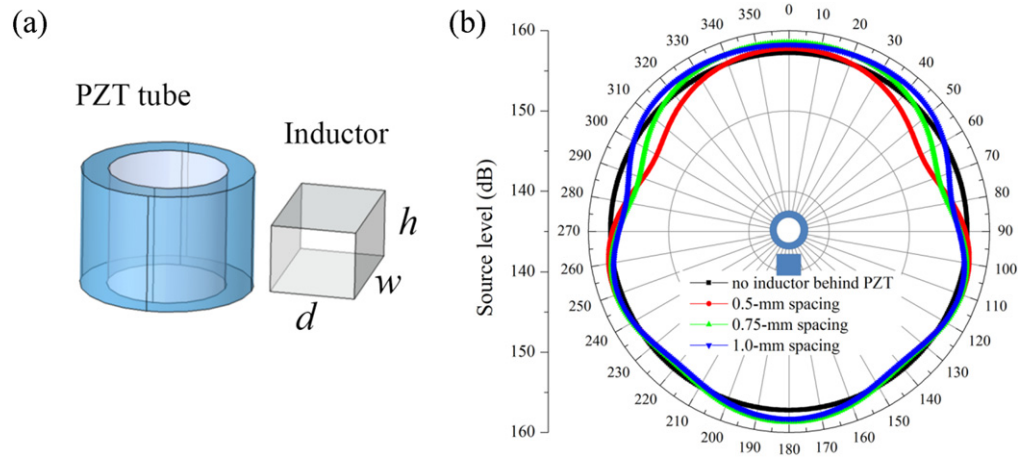

Figure 6. The PZT-inductor model used in the FE analysis (a) and the simulated beam patterns using the model with the PZT-inductor spacing setting to 0.5 mm, 0.75 mm, and 1.0 mm (b). The tube and the inductor at the center of the beam pattern indicate their relative positions.

beam pattern. Therefore, it is conceivable that the spacing between the PZT and the inductor could have a significant impact on the shape of the beam pattern.

Because of the difficulty in approaching this situation analytically (i.e. the incident cylindrical wave and the rectangular box instead of the incident plane wave and the sphere, respectively), a numerical simulation based on the FE method was conducted to verify this conjecture. The simulated beam patterns (figure 6) showed that in the top half of the beam pattern, there were marked sound pressure reductions as the transducer rotated away from 0°. This was especially pronounced at the 0.5 mm spacing setting. As the spacing was increased, the reduction was less severe while there was still some on the sides of the transducer. The SL_{avg} of the 0.5 mm spacing model was 1.5 dB lower than that of the 1.0 mm spacing model. The less severe fluctuation in the beam pattern due to the increased spacing can be qualitatively expected based on the infinite spacing for which the omnidirectional beam pattern would be achieved.

Actual transducer samples were also fabricated with the PZT-inductor spacing set to approximately 0.5 mm and 1.0 mm for beam pattern testing to compare with the simulated results. The beam patterns of the two samples (figure 7) were tested by driving the PZT transducer using the same driving voltage. It can be seen that in the top half of the beam pattern, the sample with 0.5 mm spacing exhibited source level drop on the two sides (30° to 80° and 290° to 340°) of the beam pattern, whereas the sample with 1.0 mm spacing had a much more uniform source-level readings throughout the front 180°. These results were consistent with those from the simulation. This resulted in a difference of 1.2 dB in SL_{avg}, which also is consistent with the difference predicted by the FE analysis. It should be noted that the discrepancy between the simulation and the experimental result in the back side of the PZT is due to the fact that the cable connected to the PZT was not modeled in the simulation.

3.4. Frequency tuning using a tuning inductor

Although the dimensions of the PZT transducer for the injectable transmitter can be determined based on its hoop-mode frequency constant and the 416.7 kHz application frequency, in reality, however, the OD and ID of the PZT tube vary as a result of the manufacturing tolerances, which consequently affect the actual resonance frequency of the PZT. To minimize this variation, a tuning inductor is connected in series with the PZT to create a resonance at 416.7 kHz (f_0). The inductance value of this tuning inductor was determined by using the equivalent circuit of the PZT.

A piezoelectric acoustic transducer near resonance can be approximated using an equivalent circuit (the circled portion in figure 8) [20]. The $L_1C_1R_1$ arm represents the mechanical resonance of the PZT, and C_0 and R_e are the clamped capacitance and loss of the PZT, respectively. For the injectable transmitter, the values of L_1, C_0, and C_1 can be obtained using the capacitance of the PZT (C_{PZT}) measured at a low (1 kHz) and the actual resonance frequency (f_r) and anti-resonance frequency (f_a) of the PZT measured underwater:

$$C_{PZT} = C_0 + C_1, \tag{4}$$

$$\frac{C_1}{C_{PZT}} = 1 - \left(\frac{f_r}{f_a}\right)^2, \tag{5}$$

$$\left(2\pi f_r\right)^2 = \frac{1}{L_1 C_1}. \tag{6}$$

The average measured R_1, f_r and f_a for the PZT transducer in underwater conditions were 294 Ω , 389 kHz, and 423 kHz, respectively, and the C_{PZT} for the IC-offset PZT used in this study was typically 1.20 nF. Therefore, using equations (4), (5), and (6), it can be shown that $C_0 = 1.01$ nF, $C_1 = 0.19$ nF, and $L_1 = 904$ μH. To achieve a resonance at 416.7 kHz using the tuning inductor, the imaginary part of the total impedance of the circuit should be zero at that

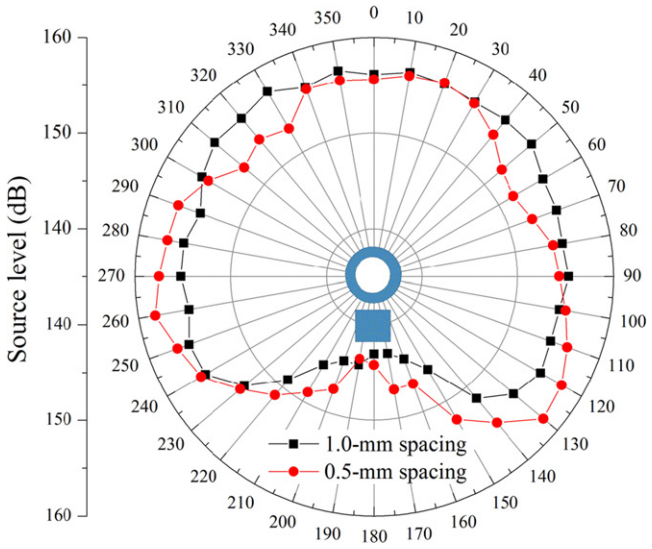

Figure 7. Experimental results of the beam patterns of the PZT tube transducer with an inductor directly behind it at two different spacings. The tube and the inductor at the center of the beam pattern indicate their relative positions.

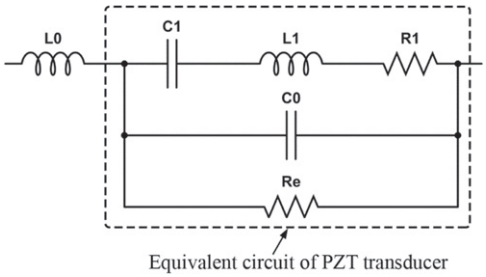

Figure 8. Equivalent circuit of the PZT transducer with a tuning inductor connected in series.

frequency. Therefore, L_0 was calculated to be 95 μH. To verify this result, the source levels of an IC-offset PZT transducer connected with a tuning inductor of various inductance values were also measured at 416.7 kHz. The source level of the transducer was found to decrease as the inductance value was changed away from 100 μH (figure 9). Because of the limited size options of commercial inductors, only inductors of inductance values of up to 100 μH could fit inside the extremely compact package of the injectable JSATS transmitter. Therefore, an inductor of 100 μH, the closest to 95 μH, was chosen as the frequency tuning inductor.

4. Conclusions

Several aspects of the PZT transducer design for a miniaturized injectable acoustic transmitter were investigated to achieve similar acoustic performance to that of the existing transmitters in a significantly smaller and lighter package. The study focused on methods that direct more of the input energy to the front half of the PZT transducer to improve the detection probability. These methods include using an IC-offset PZT tube transducer and attaching EPDM-CCF as an acoustic reflector to the back of the PZT. We found that a novel off-center tube transducer improved the average source level of the front half of the transducer by 1.5 dB. The acoustic reflector improved it by 1.3 dB. We found that too small a gap between the transducer and the component placed behind it resulted in distortion of the beam pattern. To achieve a consistent resonance and an optimal source level at the application frequency, a 100 μH inductor also was connected in series with the PZT. The findings of this work and the combination of these techniques contributed to the successful development of the new injectable transmitter.

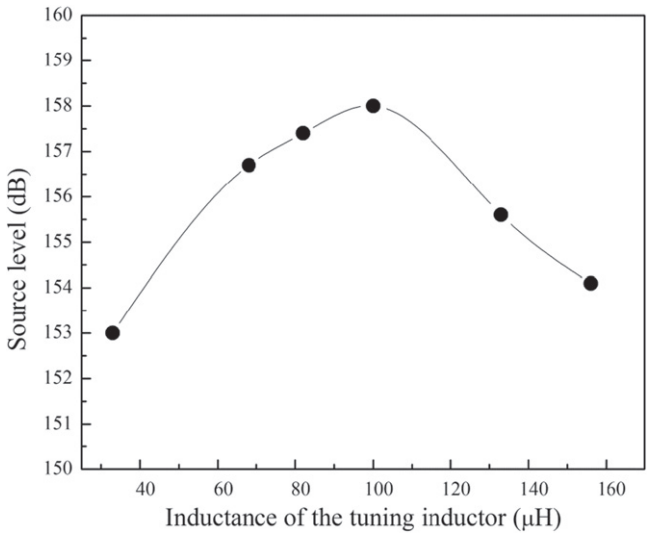

Figure 9. Source level of the transmitter as a function of the inductance value of the tuning inductor.

Acknowledgments

This study was funded by the US Army Corps of Engineers, Portland District. Brad Eppard was the technical point of contact for USACE-Portland, and we greatly appreciate his involvement and oversight. The authors would like to thank Jun Lu, Chuan Tian, and Yong Yuan for their assistance in electrical and source-level measurements and Jayson Martinez for his help in creating CAD models.

References

[1] Macilwain C 1997 Sceptics and salmon challenge scientists *Nature* **385** 668
[2] Wakefield J 2001 Record salmon populations disguise uncertain future *Nature* **411** 226
[3] Lovett R A 1999 As salmon stage disappearing act, dams may too *Science* **284** 574–5
[4] Rutz G L, Sholtis M D, Adams N S and Beeman J W 2014 *Investigation of Methods for Successful Installation and Operation of Juvenile Salmon Acoustic Telemetry Systems (JSATS) Hydrophones in the Willamette River, Oregon, 2012* US Department of the Interior & US Geological Survey

[5] Rechisky E L, Welch D W, Porter A D, Jacobs-Scott M C and Winchell P M 2013 Influence of multiple dam passage on survival of juvenile Chinook salmon in the Columbia River estuary and coastal ocean *Proc. Natl Acad. Sci.* **110** 6883–8
[6] McMichael G A, Eppard M B, Carlson T J, Carter J A, Ebberts B D, Brown R S, Weiland M, Ploskey G R, Harnish R A and Deng Z D 2010 The juvenile salmon acoustic telemetry system: a new tool *Fisheries* **35** 9–22
[7] Deng Z D, Carlson T J, Li H, Xiao J, Myjak M J, Lu J, Martinez J J, Woodley C M, Weiland M A and Eppard M B 2015 An injectable acoustic transmitter for juvenile salmon *Sci. Rep.* **5** 8111
[8] Chen H *et al* 2014 Micro-battery development for juvenile salmon acoustic telemetry system applications *Sci. Rep.* **4** 3790
[9] Deng Z Q, Weiland M, Carlson T and Eppard M B 2010 Design and instrumentation of a measurement and calibration system for an acoustic telemetry system *Sensors* **10** 3090–9
[10] Marburg S 2002 Six boundary elements per wavelength: is that enough? *J. Comput. Acoust.* **10** 25–51
[11] Berenger J-P 1994 A perfectly matched layer for the absorption of electromagnetic waves *J. Comput. Phys.* **114** 185–200
[12] Zampolli M, Nijhof M J J, de Jong C A F, Ainslie M A, Jansen E H W and Quesson B A J 2013 Validation of finite element computations for the quantitative prediction of underwater noise from impact pile driving *J. Acoust. Soc. Am.* **133** 72–81
[13] Zampolli M, Tesei A, Jensen F B, Malm N and Blottman J B 2007 A computationally efficient finite element model with perfectly matched layers applied to scattering from axially symmetric objects *J. Acoust. Soc. Am.* **122** 1472–85
[14] Shirron J J and Giddings T E 2006 A finite element model for acoustic scattering from objects near a fluid–fluid interface *Comput. Methods Appl. Mech. Eng.* **196** 279–88
[15] COMSOL 2013 *Acoustic Module 4.3b User's Guide* (Burlington, MA: COMSOL, Inc.) pp 113–5
[16] Pierce A D 1989 *Acoustics: An Introduction to Its Physical Principles and Applications* (Woodbury, NY: Acoustical Society of America) pp 180–2
[17] Kinsler L E, Frey A R, Coppens A B and Sanders J V 2000 *Fundamentals of Acoustics* (New York: Wiley) pp 149–52
[18] Li H D, Deng Z D, Yuan Y and Carlson T J 2012 Design parameters of a miniaturized piezoelectric underwater acoustic transmitter *Sensors* **12** 9098–109
[19] Postema M 2011 *Fundamentals of Medical Ultrasonics* (Boca Raton, FL: CRC Press) p 139
[20] Stansfield D 1991 *Underwater Electroacoustic Transducers* (San Altos Hills, CA: Peninsula Publishing) p 81